Phase selection and intermittency of exciton-polariton condensates in one-dimensional periodic structures

Sukjin Yoon,[1,2] Meng Sun,[1,3] Yuri G. Rubo,[1,4] and Ivan G. Savenko[1,3]

[1]*Center for Theoretical Physics of Complex Systems, Institute for Basic Science, Daejeon 34126, Korea*

[2]*School of Computational Sciences, Korea Institute for Advanced Study, Seoul 02455, Korea*

[3]*Basic Science Program, Korea University of Science and Technology, Daejeon 34113, Korea*

[4]*Instituto de Energías Renovables, Universidad Nacional Autónoma de México, Temixco, Morelos 62580, Mexico*

(Received 7 June 2018; revised manuscript received 9 June 2019; published 12 August 2019)

An exciton-polariton condensate loaded in a single active miniband in a one-dimensional microcavity wire with a complex-valued periodic potential changes its state with an increase of the polariton-polariton repulsion. This effect depends on the type of the single-particle dispersion of the miniband, which can be fine tuned by the real and imaginary components of the potential. As a result, the condensate can be formed in a zero state, π state, or mixed state of spatiotemporal intermittency, depending on the shape of the miniband, strength of interparticle interaction, and distribution of gain in the system. The change of the condensate wave function with increasing interaction takes place by proliferation of dark solitons, which are the building blocks of the new condensate phase. We show that, in general, the interacting polaritons are not condensed in the state with minimal losses, nor do they accumulate in the state with a well-defined wave vector.

DOI: 10.1103/PhysRevA.100.023609

I. INTRODUCTION

Since the discovery of superfluid–Mott insulator transition with cold atoms in optical lattices [1,2], the system of bosons in periodic potentials has attracted much attention for both fundamental and applied reasons. While the cold atoms in periodic optical lattices are probably the cleanest system, they have extremely low critical temperature due to heavy atomic masses. Exciton polaritons (polaritons) in semiconductor microcavities [3–5] possess substantially smaller effective masses and can condense not only at liquid helium [6–8] but also up to room temperature [9,10]. This makes a system of polaritons in artificial periodic potentials an excellent alternative platform for studying many-body physics, gap solitons [11,12], topological polariton states [13,14], as well as classical [15] and quantum [16] simulators.

The physics of polariton condensation is quite different from traditional cold atoms. An external pumping (coherent or incoherent) is required to create and maintain polaritons due to their finite lifetime in the microcavity, which usually prevents the particles from reaching thermal equilibrium, so that the steady-state condensate can be formed in an excited state with many-body correlations. In particular, for polariton condensates in periodic potentials, condensation at the edges of the Brillouin zone, namely, π condensation in one-dimensional (1D) lattices [8] and p and d condensation in two-dimensional (2D) lattices [17], as well as mixed condensates [18], have been observed.

Loading cavity photons and quantum-well excitons into separate periodic potentials, one can achieve multivalley (instead of π or zero) condensation [19]. Moreover, polariton condensation in the presence of distributed gain and loss of the single-particle states is expected to be accompanied by formation of spontaneous currents [20]. Another significant recent finding is the flat band condensation in 1D [21] and 2D periodic systems [22–24]. Such condensates exhibit strong enhancement of the effects of polariton-polariton interaction due to the reduced kinetic energy of the particles.

In this paper, we consider a 1D polariton system in a complex-valued (later *complex*) periodic potential and account for polariton-polariton interaction and gain saturation nonlinearity. We show that for the detailed description of the system it is necessary to consider the imaginary part of the periodic potential, which describes the distributed gain and losses [25] of single-particle states in the microcavity. By carefully choosing the parameters of the complex potential (such as height and width of its imaginary part), we can control the state of the system and demonstrate that several conceptually different situations are possible.

In the case of relatively large width of the miniband (large energy difference between the zero and π states of the single-particle spectrum), we find that the condensate changes from zero state to π state (or vice versa) with the increasing interaction between the particles. This counterintuitive effect takes place since the condensate with maximal gain becomes unstable in the case of strongly interacting particles, and the bosons accumulate in the state with a minimal gain. Consequently, the total number of particles in the condensate is not maximized.

The crossover from zero to π condensate (or vice versa) happens by formation of propagating dark solitons, which is another surprising result. At certain magnitude of the effective interaction between the particles, comparable with the bandwidth, and as a result of soliton propagation, the polaritons are distributed quasihomogeneously along the dispersion curve instead of the usual condensation that tends to accumulate the particles in a single quantum state. The polaritons occupy the band more or less uniformly, and short correlations

in space and time manifest intermittency of the condensate state.

The paper is organized as follows. In Sec. II below we introduce the generalized Ginzburg-Landau model to describe the exciton-polariton condensate in 1D complex-valued periodic potentials and give a brief description of the cases on which we will focus in our numerical simulations. In Sec. III, the simulation results are presented and discussed, and Sec. IV contains conclusions.

II. THEORETICAL MODEL

We study the solutions to the 1D generalized Ginzburg-Landau equation (GLE):

$$i\hbar\partial_t\psi = -\frac{\hbar^2}{2m^*}\partial_x^2\psi + V(x)\psi + (\alpha - i\beta)|\psi|^2\psi, \quad (1)$$

where $\psi(x,t)$ is the wave function of the polariton condensate, $V(x) = V(x+a)$ is the complex periodic potential with the lattice period a, m^* is the polariton effective mass, α is the polariton-polariton interaction constant [26–28], and $\beta > 0$ accounts for the gain-saturation nonlinearity of the system [29,30]. By scaling the wave function $\psi \to \psi/\sqrt{\beta}$, one can set $\beta = 1$, obtaining the dimensionless interaction constant α/β.

The usefulness of the generalized GLE (1) lies in (i) its simple form, as compared to more detailed descriptions involving the incoherent exciton reservoir, and (ii) its minimal set of parameters, which allows us to obtain good qualitative insight into the physics of exciton-polariton condensation in the periodic potential. We note that when the system reaches a steady state on long time scales the interaction and dissipative parameters get rescaled, taking into account the reservoir steady state. However, the general form of Eq. (1), namely, the periodicity of the potential and the presence of two nonlinearities (interaction and dissipation), remains unchanged, which is a great benefit of the Ginzburg-Landau approach. Equation (1) of our model has another advantage that it can be easily compared with the complex Ginzburg-Landau equation without a periodic potential, which is the well-established model for the study of nonlinear phenomena in different areas of physics (see, e.g., Ref. [31] for a review).

We describe the complex potential $V(x) = V_R(x) + iV_I(x)$ as a superposition of square wells in both real and imaginary parts of it, but with different widths. Namely, within the unit cell, $0 \leqslant x < a$, we have (see Fig. 1, upper panels)

$$V_R(x) = U\,\Theta\left(\left|x - \frac{a}{2}\right| - \frac{a_R}{2}\right), \quad (2a)$$

$$V_I(x) = W\,\Theta\left(\frac{a_I}{2} - \left|x - \frac{a}{2}\right|\right) - \Gamma, \quad (2b)$$

where $\Theta(x)$ is the Heaviside step function, U is the height of potential barriers, W describes the local gain, and Γ defines the uniform losses in the system (due to finite polariton lifetime in the microcavity wire). Parameters a_R and a_I are the widths of real potential wells and imaginary potential barriers, respectively.

Complex potential (2) reflects the experimental situation when the system is pumped from the excitonic reservoirs created in the barriers. Due to exciton-polariton repulsion, the particles move into the wells (similar to the case of 2D lattices of trapped polariton condensates [15]), so that the gain part of the potential (parameter W) is located at the wells. The excitonic reservoirs also increase the barrier heights. It should be noted that a uniform wire subject to a periodic pumping with the period a is described by the same model (2). This pumping produces not only periodic gain (periodic imaginary part) but also periodic repulsive potential (periodic real part). This setup has the clear benefit that the period a can be tuned. Since the gain is maximized in the potential wells, the zero state, which mainly resides in the wells, has usually bigger gain than the π state, which mainly resides in the barriers.

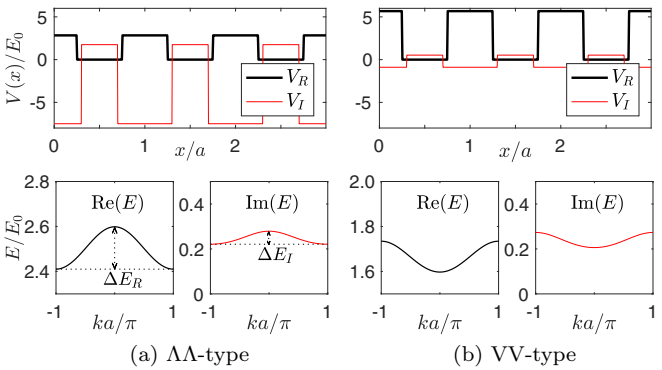

(a) ΛΛ-type (b) VV-type

FIG. 1. Complex potentials and dispersion of the first miniband. The real parts are plotted with thick black lines; the imaginary parts are plotted with thin red lines. (a) ΛΛ case: $U = 14(\hbar^2/m^*a^2)$, $W = 3.26\,U$, $\Gamma = 2.64\,U$. (b) VV case: $U = 28(\hbar^2/m^*a^2)$, $W = 0.25\,U$, $\Gamma = 0.16\,U$. The energy bandwidth ratio $\Delta E_R/\Delta E_I \approx 3$ (a) and 2 (b). In both cases, $a_R = 0.5a$ and $a_I = 0.4a$. The energies are measured in the units of $E_0 = \pi^2\hbar^2/2m^*a^2$.

It is important that depending on the values of the parameters of potential (2) the single-polariton spectrum [obtained setting $\alpha = \beta = 0$ in Eq. (1)] can be of four qualitatively different types. We classify them as ΛΛ [see Fig. 1(a), lower panel], VV [Fig. 1(b), lower panel], VΛ, and ΛV, depending on the position of the minimum of the energy (the real part of the eigenvalue) and the position of the minimum of the gain (the imaginary part of the eigenvalue) for the first miniband. For example, the ΛΛ type corresponds to the case when the minimum energy and minimum gain are both at the edge of the first Brillouin zone at $k = \pm\pi/a$ [see Fig. 1(a)]. We also can define effective widths of the bands, ΔE_R and ΔE_I.

In what follows, we will consider the formation of the polariton condensate near the threshold, when the losses in the system, governed by the parameter Γ, are big enough, and the first miniband only possesses the positive imaginary part of the eigenvalues, so that the particles are expected to condense into this miniband. The complex potential in Fig. 1 is then chosen by the following two principles: (i) Detuning the width and depth of the well to get the ground-state dispersion with the ΛΛ (or VV) type and (ii) changing the magnitude of the overall shift for the imaginary part, Γ, we make the first miniband the only band with the positive imaginary part of the eigenvalues. We also consider the first miniband to be well separated from the other bands, thus disregarding the transitions between bands.

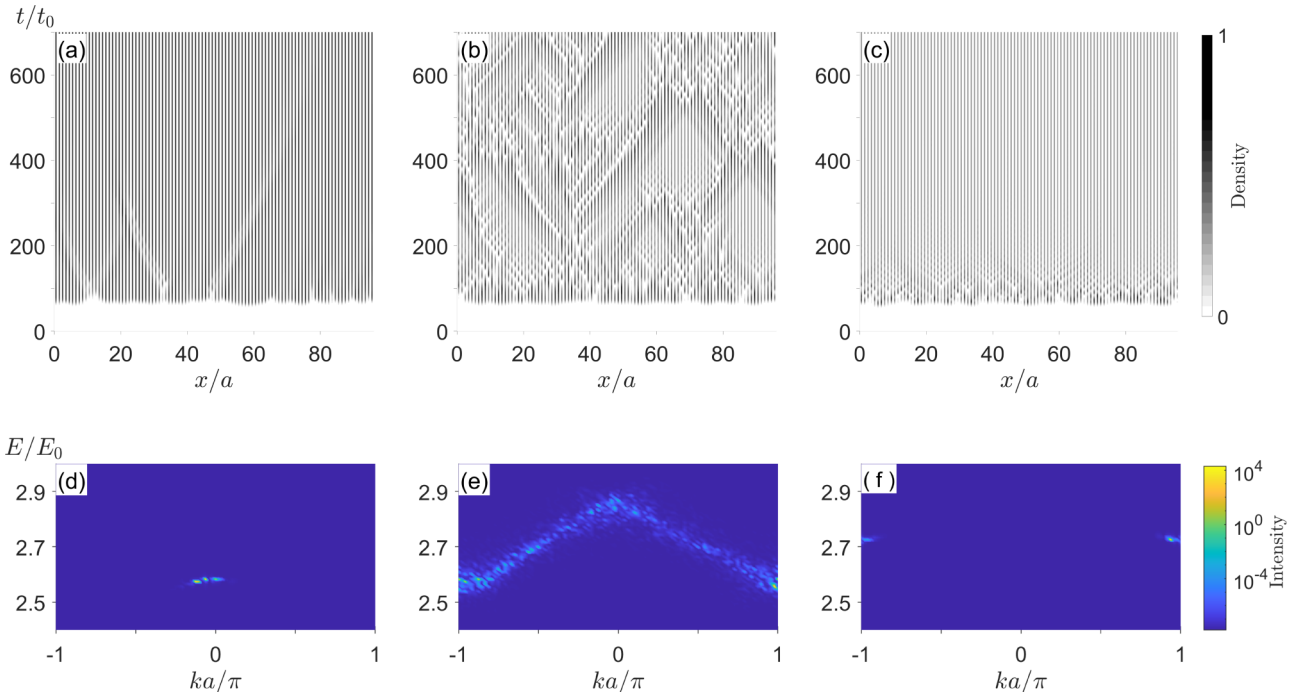

FIG. 2. Spatiotemporal pattern of the condensate density $|\psi(x,t)|^2$ (a, b, c) and intensity $|\psi(k,E)|^2$ (d, e, f) for the $\Lambda\Lambda$ case. $\alpha/\beta = 0$ (a, d), 2 (b, e), and 6 (c, f). Time is measured in units of $t_0 \equiv \hbar/E_0$.

III. RESULTS AND DISCUSSION

A. Spatiotemporal dynamics of the condensate

For noninteracting polaritons one expects to obtain their condensate in the state with the maximal gain. Thus the number of particles is maximized in this state and it is stabilized by finite gain-dissipation parameter β. Therefore, we expect the zero-state condensation in $\Lambda\Lambda$ and VΛ cases, and π-state condensation in ΛV and VV cases. Numerical solutions of Eq. (1) show that this scenario remains valid even in the presence of strong repulsion between polaritons in the VΛ and ΛV cases. However, the polariton-polariton interaction has a dramatic effect on the condensate loaded in the $\Lambda\Lambda$ and VV minibands, leading to fundamental reconstruction of the condensate state with the increase of interactions. Therefore we will mostly concentrate on the VV and $\Lambda\Lambda$ configurations.

Figures 2 and 3 show spatiotemporal dynamics of the condensate for the $\Lambda\Lambda$ and VV cases. The upper rows of these figures show spatiotemporal patterns of the condensate density $|\psi(x,t)|^2$ and the lower rows show the polariton emission intensities $|\psi(k,E)|^2$ for a small initial random seed of noise. We calculated 50 trajectories and checked that different small initial random seeds give a qualitatively similar picture. In density plots, shown in panels (a), (b), and (c), the local maxima of the condensate density (dark black vertical lines along the time axis) are at the centers of wells of the real potential V_R, where the maximal gain is attained [see also Figs. 6(a) and 6(b)].

Going right from panels (a) and (d) to panels (c) and (f) in Figs. 2 and 3, the dimensionless parameter α/β increases and we observe considerable changes in the spatiotemporal density patterns and condensation states. (a, d) When $\alpha/\beta = 0$, the condensate is formed in the state with the maximal gain: the zero state in the $\Lambda\Lambda$ case and the π state in the VV case. The defects appearing at the early stage of evolution dissipate away at later times. In panels (b) and (e), when α/β takes an intermediate value, polaritons no longer accumulate in the state with a well-defined wave vector, but rather they distribute along the whole miniband. As one can see from panels (b), strong spatiotemporal chaos is present in this case. In panels (c) and (f), surprisingly, with further increase of α/β, the well-defined condensation takes place again, but now the condensate is formed at the minimum of the dispersion, in the state with the smallest gain. It corresponds to the π state in the $\Lambda\Lambda$ case and the zero state in the VV case. This result is in contrast with the one obtained in the zero interaction regime [compare panels (d) and (f)]. It should be noted that the π state in our system is different from the one discussed in Ref. [8], where it corresponds to the minimum of the second miniband.

The density patterns presented in panels (b) resemble those of spatiotemporal intermittency in the 1D complex Ginzburg-Landau equation (CGLE) [32–34], which can be written in the form

$$i\partial_t A = iA + (c_1 + i)\partial_x^2 A + (c_3 - i)|A|^2 A. \tag{3}$$

The nonlinear term here takes the same form as in Eq. (1) and the linear terms for $c_1 > 0$ correspond to the complex-valued energy dispersion of $\Lambda\Lambda$ type even though the dispersion in Fig. 1 is not a quadratic but a periodic function. The parameters c_1 and c_3 play similar roles as $\Delta E_R/\Delta E_I$ and α/β in our system, respectively. However, the shapes of real and imaginary parts of the dispersion in Fig. 1 are not exactly proportional to each other and the *continuous* translation symmetry of CGLE is reduced to a *discrete lattice* translation symmetry due to the periodic potential.

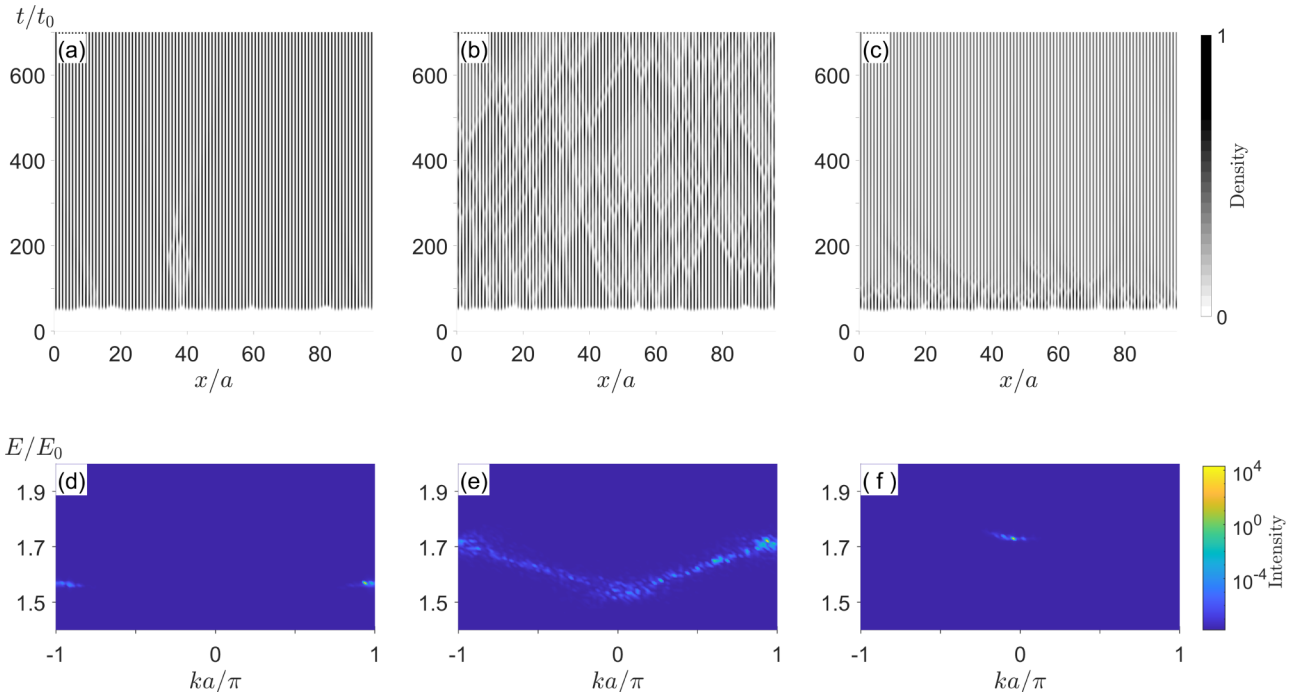

FIG. 3. Spatiotemporal pattern of the condensate density $|\psi(x,t)|^2$ (a, b, c) and intensity $|\psi(k,E)|^2$ (d, e, f) for the VV case. $\alpha/\beta = 0$ (a, d), 0.65 (b, e), and 2 (c, f).

There is also another important difference. Even though the offset term iA in Eq. (3) admits only a restricted range of wave numbers ($-1 < k < 1$) to have a positive gain with a maximum at $k = 0$, the edge points $k = \pm 1$ have *zero* gain, and therefore the condensate cannot be formed at the edge. Instead, the polariton system is characterized by edge points of the first Brillouin zone $k = \pm\pi/a$ with *finite* gain and the singularity in the density of states. It is this feature that leads to the possibility of formation of the polariton condensate at the edge.

In the system described by the CGLE, the spatiotemporal intermittent phase appears in the transition from a plane-wave to a turbulent (chaotic) state [32]. In our case, the phase landscape is different: a zero-state Bloch wave, a π-state Bloch wave (instead of the turbulent state), and the spatiotemporal intermittency which separates these states. Nonetheless, the spatiotemporal intermittency pattern is quite similar to the conventional one. We note that the intermittency phase exhibits some features of the deterministic chaos within a single trajectory. Similar intermittent polariton states have recently been reported in spontaneously formed periodic structures under resonant driving [35].

The crossover from the spatiotemporal intermittent dynamics to the π condensate in the $\Lambda\Lambda$ case (or to the zero condensate in the VV case) is not always possible. The formation of a new condensate phase depends not only on the polariton interaction strength α/β, as has been discussed above, but also on the ratio $\Delta E_R/\Delta E_I$. Figure 4 demonstrates (for the $\Lambda\Lambda$ case) that a sufficiently large value of the ratio $\Delta E_R/\Delta E_I$ is required to reach a π state from the mixture state of the spatiotemporal intermittency.

B. Spatiotemporal intermittency

It has been suggested that the transition from a laminar (regular) state to the turbulent (irregular) state via spatiotemporal intermittency can be related to the directed-percolation process [36]. Following directed percolation studies, one can quantify spatial intermittency by measuring the distribution of the lengths of laminar domains, which is expected to reveal a power-law behavior at the spatiotemporal intermittency threshold [37,38].

The spatiotemporal patterns which we observe are not exactly the same as in the conventional spatiotemporal intermittency [36]. In our system, the spatiotemporal intermittent pattern appears halfway between two ordered phases (zero and π phases). On both sides of intermittency domain there is only one stable condensate state (single stable attractor). Inside the intermittency domain, both zero and π phases of the condensate are stable, but they possess different basins of attraction. The basin of attraction of the new phase grows with increasing polariton-polariton interaction, and the basin of attraction of the old phase shrinks down. Near the boundary of the intermittency domain, the phase with a smaller basin of attraction is manifested by the propagating solitons, which have the form of small domains of this less-probable phase. More detailed analysis involves studying the sizes of basins of attraction and the Lyapunov exponents of the two phases in question and it is beyond the scope of this paper.

However, the spatiotemporal pattern in our case is quite similar to the one appearing in the transition to turbulence. We also consider the distribution of lengths of the defect domains, which represent domains of dark solitons in both $\Lambda\Lambda$ and

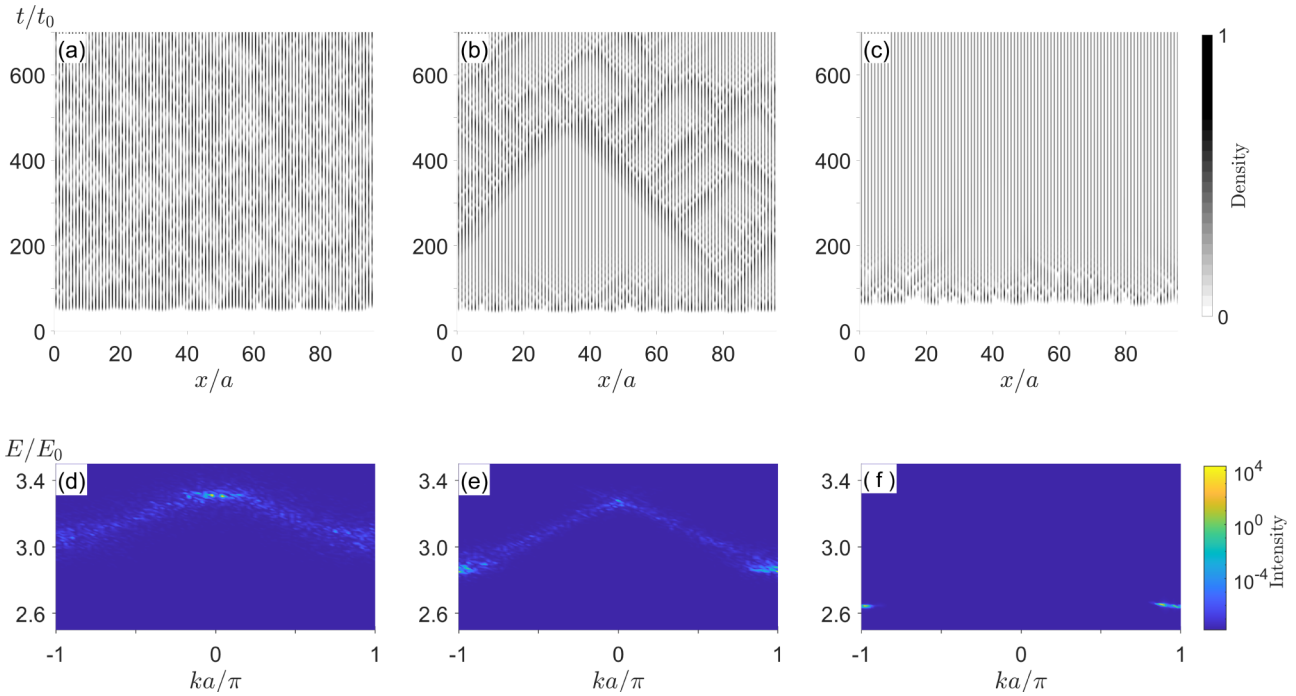

FIG. 4. Spatiotemporal pattern of the condensate density $|\psi(x,t)|^2$ (a, b, c) and intensity $|\psi(k,E)|^2$ (d, e, f) for the $\Lambda\Lambda$ cases with $\alpha/\beta = 4$ fixed. The ratios of the real and imaginary parts of the energy bandwidths are $\Delta E_R/\Delta E_I \approx 1$, 2, and 4 from (a, d) to (c, f). $W = 3.82\,U$ (a, d), $3.43\,U$ (b, e), and $3.18\,U$ (c, f) with $U = 14(\hbar^2/m^*a^2)$. $\Delta E_R \approx 0.107\,E_0$ (a, d), $0.164\,E_0$ (b, e), and $0.201\,E_0$ (c, f) with $E_0 = \pi^2\hbar^2/2m^*a^2$.

VV cases. Figure 5 shows the distributions of N_L (number of defect domains of length L). Here N_L is sampled at $t/t_0 = 200 \rightarrow 700$ with the time interval of 5. We have checked that the linear decline behavior (in the log-log scale) is insensitive to the choice of smaller time intervals. We indeed observe close to power-law behavior, which is the fingerprint of the spatiotemporal intermittency.

C. Soliton dynamics

At weak polariton-polariton interaction, the long-range order of the zero condensate in the $\Lambda\Lambda$ case and the π condensate in the VV case is destroyed by formation of propagating defects. Each defect extends only over a few lattice constants, and it is characterized by the suppression of the condensate occupation and by the phase slips.

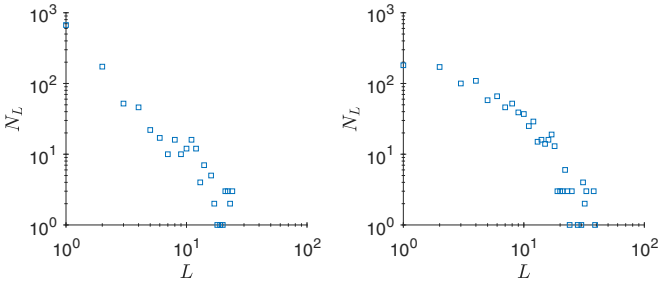

(a) $\Lambda\Lambda$-type (b) VV-type

FIG. 5. Distributions of the number of defect domains (N_L) for the spatiotemporal patterns, presented in Figs. 2(b) and 3(b). N_L is sampled from $t/t_0 = 200$ to 700 with the time interval of $t/t_0 = 5$. Both horizontal and vertical axes are in the log scales. The length L is in the units of lattice constant a.

As an example, Fig. 6 shows the collision events of a pair of such defects propagating towards each other. The individual collisions are seen only for weakly interacting polaritons, when the concentration of defects is small. Each defect is characterized by the depletion of the particle density together with an abrupt change in the phase of the wave function at two edge points of the defect, where the phase change is about π in the $\Lambda\Lambda$ case, while the phase change is smooth in the VV

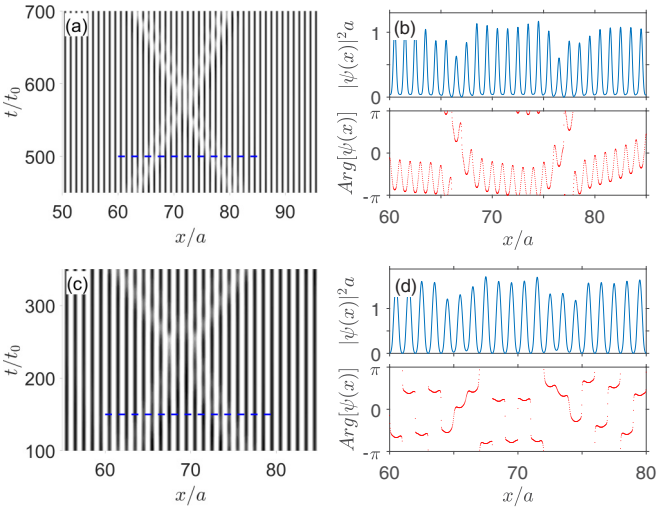

FIG. 6. Propagation and collision of a pair of solitons in the $\Lambda\Lambda$ case (a, b) and VV case (c, d) for $\alpha/\beta = 0.4$, when the number of solitons is small. (b, d) The upscaled profiles of the particle density and the phases of the wave functions just before the collision [along the thick dashed blue lines in panels (a, c), respectively].

case. The fact that the defects maintain their properties after the collision indicates that they can also be considered as dark solitons. We note, however, that these solitons are different from the Bekki-Nozaki hole solutions of CGLE [39] or the dissipative Gross-Pitaevskii equation for the polariton mean field [40]. In our case, solitons represent the building blocks of a new condensate phase.

The density of solitons increases with α/β, and some of them attach to each other, forming wide soliton domains, which one can see in Figs. 2(b) and 3(b). In the $\Lambda\Lambda$ case, with further increase of polariton-polariton interaction and for sufficiently large ratio $\Delta E_R/\Delta E_I$, a complete array of dark solitons is formed as in Fig. 2(c). The wave-function phase changes by π per every lattice constant and the quasi-long-range order appears again, manifesting the formation of the π-condensate phase.

IV. CONCLUSIONS

Interacting exciton polaritons loaded into a one-dimensional microcavity wire with a periodic potential and periodic distribution of losses can condense into nontrivial states, where losses are not minimized but maximized. Under certain conditions, polaritons can form a space-time intermittency phase, which separates two condensate phases with minimal and maximal losses. The reconstruction of the condensate wave function takes place by proliferation of dark solitons along the periodic structure. The nuclei of the new condensate phase, which are characterized by maximization of losses, are formed with increasing polariton-polariton interaction, and they can be seen as a result of gluing the dark solitons together.

ACKNOWLEDGMENTS

We thank Boris Altshuler, Alexey Andreanov, and Sergej Flach for useful discussions. The authors acknowledge the support of the Institute for Basic Science in Korea (Project No. IBS-R024-D1). Y.G.R. acknowledges support from CONACYT (Mexico) under Grant No. 251808.

[1] D. Jaksch, C. Bruder, J. I. Cirac, C. W. Gardiner, and P. Zoller, Phys. Rev. Lett. **81**, 3108 (1998).
[2] M. Greiner, O. Mandel, T. Esslinger, T. W. Hänsch, and I. Bloch, Nature (London) **415**, 39 (2002).
[3] C. Weisbuch, M. Nishioka, A. Ishikawa, and Y. Arakawa, Phys. Rev. Lett. **69**, 3314 (1992).
[4] H. Deng, G. Weihs, C. Santori, J. Bloch, and Y. Yamamoto, Science **298**, 199 (2002).
[5] A. Kavokin, J. Baumberg, G. Malpuech, and F. Laussy, *Microcavities*, Series on Semiconductor Science and Technology (Oxford, New York, 2007).
[6] J. Kasprzak, M. Richard, S. Kundermann, A. Baas, P. Jeambrun, J. M. J. Keeling, F. M. Marchetti, M. H. Szymańska, R. André, J. L. Staehli, V. Savona, P. B. Littlewood, B. Deveaud, and L. S. Dang, Nature (London) **443**, 409 (2006).
[7] R. Balili, V. Hartwell, D. Snoke, L. Pfeiffer, and K. West, Science **316**, 1007 (2007).
[8] C. W. Lai, N. Y. Kim, S. Utsunomiya, G. Roumpos, H. Deng, M. D. Fraser, T. Byrnes, P. Recher, N. Kumada, T. Fujisawa, and Y. Yamamoto, Nature (London) **450**, 529 (2007).
[9] J. J. Baumberg, A. V. Kavokin, S. Christopoulos, A. J. D. Grundy, R. Butté, G. Christmann, D. D. Solnyshkov, G. Malpuech, G. Baldassarri Höger von Högersthal, E. Feltin, J.-F. Carlin, and N. Grandjean, Phys. Rev. Lett. **101**, 136409 (2008).
[10] G. Lerario, A. Fieramosca, F. Barachati, D. Ballarini, K. S. Daskalakis, L. Dominici, M. De Giorgi, S. A. Maier, G. Gigli, S. Kéna-Cohen, and D. Sanvitto, Nat. Phys. **13**, 837 (2017).
[11] D. Tanese, H. Flayac, D. Solnyshkov, A. Amo, A. Lemaître, E. Galopin, R. Braive, P. Senellart, I. Sagnes, G. Malpuech, and J. Bloch, Nat. Commun. **4**, 1749 (2013).
[12] J. V. T. Buller, R. E. Balderas-Navarro, K. Biermann, E. A. Cerda-Méndez, and P. V. Santos, Phys. Rev. B **94**, 125432 (2016).
[13] T. Karzig, C.-E. Bardyn, N. H. Lindner, and G. Refael, Phys. Rev. X **5**, 031001 (2015).
[14] D. R. Gulevich, D. Yudin, I. V. Iorsh, and I. A. Shelykh, Phys. Rev. B **94**, 115437 (2016).
[15] H. Ohadi, A. J. Ramsay, H. Sigurdsson, Y. del Valle-Inclan Redondo, S. I. Tsintzos, Z. Hatzopoulos, T. C. H. Liew, I. A. Shelykh, Y. G. Rubo, P. G. Savvidis, and J. J. Baumberg, Phys. Rev. Lett. **119**, 067401 (2017).
[16] T. C. H. Liew and Y. G. Rubo, Phys. Rev. B **97**, 041302(R) (2018).
[17] N. Y. Kim, K. Kusudo, C. Wu, N. Masumoto, A. Löffler, S. Höfling, N. Kumada, L. Worschech, A. Forchel, and Y. Yamamoto, Nat. Phys. **7**, 681 (2011).
[18] L. Zhang, W. Xie, J. Wang, A. Poddubny, J. Lu, Y. Wang, J. Gu, W. Liu, D. Xu, X. Shen, Y. G. Rubo, B. L. Altshuler, A. V. Kavokin, and Z. Chen, Proc. Natl. Acad. Sci. USA **112**, E1516 (2015).
[19] M. Sun, I. G. Savenko, H. Flayac, and T. C. H. Liew, Sci. Rep. **7**, 45243 (2017).
[20] A. V. Nalitov, T. C. H. Liew, A. V. Kavokin, B. L. Altshuler, and Y. G. Rubo, Phys. Rev. Lett. **119**, 067406 (2017).
[21] F. Baboux, L. Ge, T. Jacqmin, M. Biondi, E. Galopin, A. Lemaître, L. Le Gratiet, I. Sagnes, S. Schmidt, H. E. Türeci, A. Amo, and J. Bloch, Phys. Rev. Lett. **116**, 066402 (2016).
[22] S. Klembt, T. H. Harder, O. A. Egorov, K. Winkler, H. Suchomel, J. Beierlein, M. Emmerling, C. Schneider, and S. Höfling, Appl. Phys. Lett. **111**, 231102 (2017).
[23] C. E. Whittaker, E. Cancellieri, P. M. Walker, D. R. Gulevich, H. Schomerus, D. Vaitiekus, B. Royall, D. M. Whittaker, E. Clarke, I. V. Iorsh, I. A. Shelykh, M. S. Skolnick, and D. N. Krizhanovskii, Phys. Rev. Lett. **120**, 097401 (2018).
[24] M. Sun, I. G. Savenko, S. Flach, and Y. G. Rubo, Phys. Rev. B **98**, 161204(R) (2018).
[25] K. Winkler, O. A. Egorov, I. G. Savenko, X. Ma, E. Estrecho, T. Gao, S. Müller, M. Kamp, T. C. H. Liew, E. A. Ostrovskaya, S. Höfling, and C. Schneider, Phys. Rev. B **93**, 121303(R) (2016).

[26] C. Ciuti, V. Savona, C. Piermarocchi, A. Quattropani, and P. Schwendimann, Phys. Rev. B **58**, 7926 (1998).
[27] F. Tassone and Y. Yamamoto, Phys. Rev. B **59**, 10830 (1999).
[28] E. B. Magnusson, I. G. Savenko, and I. A. Shelykh, Phys. Rev. B **84**, 195308 (2011).
[29] J. Keeling and N. G. Berloff, Phys. Rev. Lett. **100**, 250401 (2008).
[30] D. V. Karpov, I. G. Savenko, H. Flayac, and N. N. Rosanov, Phys. Rev. B **92**, 075305 (2015).
[31] I. S. Aranson and L. Kramer, Rev. Mod. Phys. **74**, 99 (2002).
[32] H. Chate, Nonlinearity **7**, 185 (1994).
[33] F. Melo and S. Douady, Phys. Rev. Lett. **71**, 3283 (1993).
[34] M. van Hecke, Phys. Rev. Lett. **80**, 1896 (1998).
[35] S. S. Gavrilov, Phys. Rev. Lett. **120**, 033901 (2018).
[36] Y. Pomeau, Physica D **23**, 3 (1986).
[37] H. Chaté and P. Manneville, Phys. Rev. Lett. **58**, 112 (1987).
[38] H. Chaté and P. Manneville, Spatiotemporal intermittency, in *Turbulence: A Tentative Dictionary*, edited by P. Tabeling and O. Cardoso (Springer, New York, 1994), pp. 111–116.
[39] N. Bekki and K. Nozaki, Phys. Lett. A **110**, 133 (1985).
[40] Y. Xue and M. Matuszewski, Phys. Rev. Lett. **112**, 216401 (2014).